End-Effector Guidance of Robot Arms

Yoram Koren (1) and Moshe Shoham
Received on March 2, 1987 — Accepted by the Editorial Committee

This paper deals with a robotic system in which the end-point is directly controlled. It consists of a remote guidance subsystem and a manipulator with an end-of-arm sensor subsystem. The guidance subsystem transmits and manipulates a laser beam in space, and the sensor detects the beam, sends the information to the robot controller, which, in turn, instructs the manipulator to follow the beam. The possible modifications in the manipulator structure, electronic hardware, and controller software of such systems are discussed. An experimental system consists of a SCARA-type flexible arm was constructed, and the results of the experiments are reported in the paper.

Key-Words: Robot, Flexible Arm, Manipulator Remote-Guidance.

1. Introduction

Most of the industrial robots today are programmed to do repetitive tasks, and only minor fraction are designed to adapt their motions to the changing environment [1]. Robots are capable to work in a changing environment only when they are equipped with sensors which allow the robot to update the programmed motions to the new situation. During the last decade an extensive efforts have been done to enhance the sensors capabilities and to improve their data processing. However, most of these works are directed toward the interaction between the robot and its environment, and only few works deal with the possible influence of the sensor integration on the robot structure itself. These latter works usually discuss the possible reduction of the manipulator rigidity by using a sensor to correct the arm deflections [2-4].

By contrast, in our work we have found that by employing an end-of-arm sensor and an appropriate guidance system, not only the structure of the arm can be changed, but the controller software can be modified to speed up the kinematic calculations by one order of magnitude. Utilizing the sensor, the motion control algorithm can be simplified by approximations which do not affect the accuracy since the sensor detect and correct the deviation from the required target. A broader discussion about these modifications is presented in the next section. To prove our claims we built an experimental system, the description of which is presented in Section 3. The experimental results are reported in Section 4.

2. The Sensor Effect on the Structure and Control

This section presents the possible effects of an end-effector sensing on the robot structure and its control. It is assumed that the sensor can detect the end-effector location and can guide it to the required location. The effects might be classified into three categories: manipulator, electronic hardware, and software.

A typical payload-to-weight ratio of a robot arm is about 1:20. The need to reduce the manipulator weight in order to increase the payload-to-weight ratio has been mentioned in several works [5-7], but in all these works it was assumed that the arm rigidity must not be affected. In conventional arms the actual positions are monitored at the joints and the high rigidity is required to accomplish the robot accuracy. However, when the end of the arm location is directly monitored by a sensor, the rigidity is less significant and the arm weight can be reduced. As a consequence, the structure becomes more flexible, but this does not prevent the positioning of the arm end at high accuracies.

It has been shown by the authors, that in sensor guided robots the first joint encoder can be eliminated from the robot arm [8]. Moreover, the resolution of the other encoders can be reduced, since the precise location of the end-effector is no longer determined by the encoders. Eliminating and using inexpensive encoders, reduce the cost of the arm.

Further cost reduction is achieved at the production stage. The arm manufacturing and assembly processes are done at present accurately since the computation of the end-effector location is based on the dimensions of the links and the geometric configuration (e.g., a precise 90° between two links). All the geometric errors in the manipulator are usually accumulated and resulted in a limited robot accuracy. Therefore, the tolerances in the production and assembly of conventional robots must be high. When an end-of-arm sensor is used, the production tolerances can be reduced. The sensor is used to detect and correct deviations from the required path, and the end-effector location is no longer computed by the conventional kinematic algorithm, which strongly depends on the geometry.

The utilization of the sensor affects also the controller software. It is known that one of the parameters that limits the robot performance (e.g., accuracy and response time), is the computation time required to transform the prescribed trajectory to motor commands. Extensive work has been done to reduce this time, since real-time control is essential. In conventional robots this computation must be done accurately since it affects directly the trajectory of the end-effector. However, when a sensor that detects the end-effector location is used, there is no need to derive this computation accurately because the sensor can detect and correct deviations from the required location. In this case an approximate, and hence faster, algorithm can be applied. This issue is described in detail in [8], where several approximations for the kinematic algorithm were introduced.

When a guiding system is used to control the end-effector, it is possible to divide the robot controller software into two separate parts. The programming of the path and the corresponding instructions to the end-effector are performed with one general purpose controller regardless of the specific robot that is being guided. The second controller controls the manipulator joints. The instructions to the robot in our case are given by a beam of light manipulated in space. The robot serves just as a follower to the beam motions, and consequently its controller does not contain any programming language. The computations of the required joint motor speeds performed in this controller are simpler, and all together the robot itself (including the manipulator and its control) becomes a very inexpensive unit.

3. The Experimental System

Based on the consequences of the previous discussion, an experimental end-effector guidance system was built. The system consists of a two degrees-of-freedom arm, a guidance system based on a manipulated laser beam, and an optical sensor attached to the arm end-effector.

The required task program of the robot is programmed in the guidance system controller, and translated into laser beam motions. The sensor detects the motion of the beam and sends signals to the robot controller to track the beam motion. The description of the system is depicted in Fig. 1.

The arm is a modified SCARA-type HIRATA ARH-300 robot. The second link of the HIRATA was replaced by a long (750 mm) and flexible link, and the original controller was replaced by a DEC LSI-11 microcomputer. The lowest natural frequency of the original arm was about 20 Hz, and that of the modified flexible link was about 6 Hz.

The motion control algorithm implemented in the robot controller is based on the resolved motion rate control scheme [9]. For the two degrees of freedom robot (see Fig. 2) the following equation has been used

$$\begin{bmatrix} \dot{\theta}_1 \\ \dot{\theta}_2 \end{bmatrix} = \frac{1}{L_1 L_2 S_2} \begin{bmatrix} L_2 & 0 \\ -L_2 - L_1 C_2 & L_1 S_2 \end{bmatrix} \begin{bmatrix} V_x \\ V_y \end{bmatrix} \qquad (1)$$

where $\dot{\theta}_i$ is the i-th joint speed and Vx, Vy are the required velocity components of the end-effector in the tool coordinate system.

However, there might be a possibility that the detector loses the beam. In this case a conventional motion control (utilizing the joint's feedback) is applied and the motion toward the target is continued until the communication between the detector and the laser beam is re-established. The following equation is used in this case.

$$\begin{bmatrix} \dot{\theta}_1 \\ \dot{\theta}_2 \end{bmatrix} = \frac{1}{L_1 L_2 S_2} \begin{bmatrix} L_2 C_{12} & L_2 S_{12} \\ -L_1 C_1 - L_2 C_{12} & -L_1 S_1 - L_2 S_{12} \end{bmatrix} \begin{bmatrix} V_{xw} \\ V_{yw} \end{bmatrix} \qquad (2)$$

where $C_{12} = \cos(\theta_1 + r_2)$, $S_{12} = \sin(\theta_1 + r_2)$, and V_{xw}, V_{wy} are the required velocity of the end-effector in the world coordinate system.

A block diagram of the arm controller software is shown in Fig. 3. Since a sensor is attached to the robot end-effector, the velocity commands are resolved in the tool coordinate system, and Eq. (1) becomes independent of the first joint variable (S_1 and C_1 do not appear in Eq. 1). Therefore, with this algorithm, there is no need for the first joint encoder. Moreover, the second joint encoder need not to be accurate since the precise end-effector location is determined by the sensor and not by this encoder. In the present system an encoder of 512 pulses per revolution of the joint has been used, and fairly small look-up tables for the trigonometric functions have been implemented. This enables to speed up the computation; by using Forth and Assembly languages a cycle time of 0.8 ms was achieved.

4. Experimental Results

The results of the following experiments are reported below.

1. The impulse response of the conventional arm arm and the flexible arm (with the end-effector guided system and the proposed control scheme).

2. The arm deflection to a constant load on the original rigid arm and the flexible arm.

3. Tracking the moving laser beam with the proposed system.

4. Re-establishment of a contact with the laser beam.

In all the experiments the deviation of the sensor from the required location was measured as function of time. In the first and second experiments the angle between the two links was approximately 90 degrees, and the motion was measured along the flexible axis of the second link.

4.1 The Impulse Response of the Arm The impulse response of the arm is shown in Figs. 4-6. In Fig. 4 the original controller of the arm was used, which means that the joint variables are used as the feedback to the control loops. In this experiment the joint servo are locked and there is no change in the second joint angle when the end-effector vibrates about the steady-state location. However, when the end-effector control is used (Fig. 5), this joint can move to suppress the vibration since the feedback to the control loops is supplied by the end-effector sensor. The entire settling time of the motion cannot be computed in the first case since a steady-state error was measured. Comparing the time required for the vibration amplitude to be less than 0.12 mm (0.005 inch), shows that 1.2 s are required for the conventional control and only 0.75 s for the end-effector control (although controlling a flexible arm). Moreover, the steady state error that appears in the first experiment, probably because of the backlash in the transmission, vanishes when end-effector control is used. Figure 6 shows the reference signal (motor speed command of joint 2) generated by the robot controller, as a result of the impulse excitation.

4.2 Response to a Constant Load The arm response to constant load applied at the end-effector is shown in Figs. 7-9. The load applied was 5N in the direction of the flexible axis of the second link. When the original controller was used (Fig. 7) the joint angles remain constant, but the end-effector deviates from the original position (approximately 0.6 mm). The advantages of the proposed end-effector control is demonstrated in Fig. 8. In this experiment the angles are moved so that the torque applied by the joints cancels the deviation of the end-effector. Figure 9 depicts the reference signal generated by the arm controller resulting from the external load.

4.3 Tracking the Moving Laser Beam The arm capability to track the moving laser beam was checked in this experiment. The beam starts to move from rest, and accelerates to a velocity of 0.1 m/s. The motor which manipulates the beam has a time constant of 0.01 s. Figure 10 shows the position error of the end-effector as well as the reference signal to joint 2. The error is developed to about 2 mm at the acceleration stage, and then decreases to about 0.5 mm during the motion at constant velocity.

4.4 Re-establish a Contact with the Beam In case that the sensor loses the beam, the arm moves autonomously to the final location. Close to the final location the contact with the beam is re-established. The motion toward the final location is controlled by the conventional controller, but as soon as the contact with the beam is re-established the program branches to the end-effector control algorithm. Figure 11 shows the position error of the detector and the reference signal of angle θ2. Till point A the arm moves autonomously using the conventional joint feedback control method. At point A the detector detects the beam and the end-effector control program takes over.

5. Conclusions

In this work an end-effector guided arm was constructed, and the possible changes in the arm structure and control were investigated. The arm was equipped with an optical sensor attached to the end-effector, and a guiding system that consists of a movable laser beam directed the sensor along the prescribed path. The following changes in the arm structure and control were made: The arm rigidity was reduced, the arm manufacturing tolerances were increased, the first joint encoder was eliminated, and the resolution of the other encoder was very coarse. Despite all these changes the end-effector can be located within 0.1 mm from the required point. The changes in the controller software that enabled reduction of the computation cycle time (to 0.8 ms) were based on the following ideas: Since the signals of the required motion are provided by the end-effector sensor, the motion control algorithm is computed in the tool coordinate system, and therefore became simpler. Also, since the end-effector position is corrected by the sensor, the trigonometric function and the motion algorithm can be approximated and hence computed faster.

6. References

1. Koren, Y.: Robotics for Engineers, McGraw-Hill Book Co., New York, 1985.

2. Balas, M. J.: "Feedback Control of Flexible Systems," IEEE Trans. on Automatic Control, Vol. AC-23, No. 4, August 1978, pp. 673-679.

3. Liegeois, E., et al.: "Learning and Control for a Compliant Computer-controlled Manipulator," IEEE Tran.on Automatic Control, Vol. 25, No. 6, 1980, pp. 1097-1102.

4. Schmitz, E. and Cannon, R. H.: "Initial Experiments on the End-point Control of a Flexible One-link Robot," The Int. J. Robotic Research, Vol. 3, No. 3, 1984, pp. 62-75.

5. Dubowsky, S.: "The Dynamic and Control of Robotic Manipulators," Proc. of the NATO Advanced Study, Pascoly, Italy, 1983.

6. Judd R.P and Falkenburg, D. R.: "Dynamic of Nonrigid Articulated Robot Linkages," IEEE Trans. on Automatic Control, Vol. AC-30, No. 5, May 1985, pp. 499-502.

7. Book, W.J. and Majette, M.: "Controller Design for Flexible Disturbed Parameter Mechanical Arms Via Combined State Space and Frequency Domain Techniques," ASME Trans., J. of Dynamic Systems Measurements ments and Control, Vol. 105, December 1983, pp. 245-254.

8. Shoham, M. and Koren, Y.: "Motion Control Algorithms for Sensor Equipped Robots," ASME Trans. J. of Dynamic Systems Measurements and Control, 1987.

9. Whitney, D. E.: "The Mathematics of Coordinate Control of Prosthetic Arms and Manipulators," ASME Trans. J. of Dynamic Systems Measurements and Control, December 1972, pp. 303-309.

7. Acknowledgement This research was performed at the Technion-Israel Institute of Technology under sponsorship of Elron Inc., Haifa, Israel. The authors would like to thank Dr. Zohar Ophir, V.P. for Advanced Technologies at Elron, for his active support of this research.

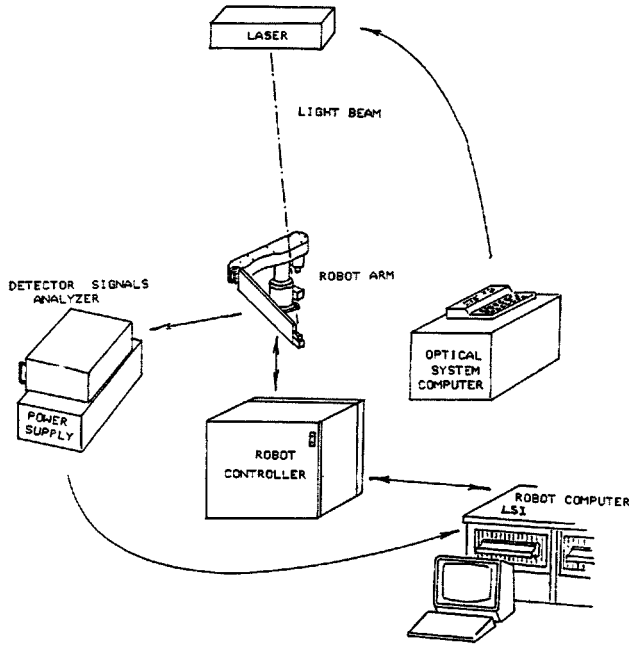

Fig. 1. The end-effector guidance system

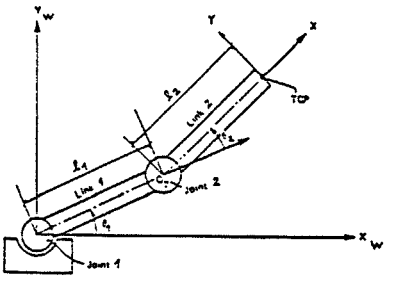

Fig. 2 Two-link planar manipulator.

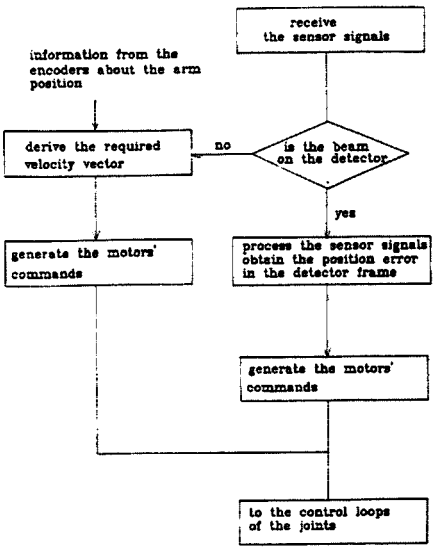

Fig. 3 Block diagram of the controller software

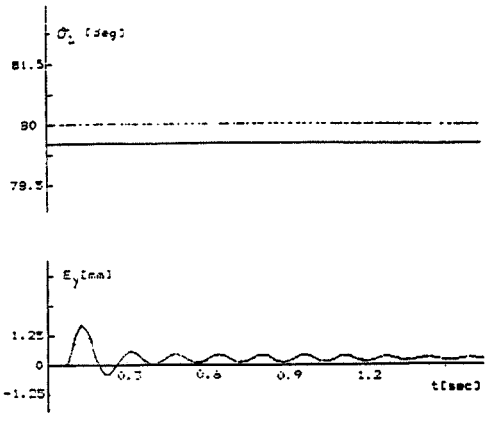

Fig. 4 The arm impulse response with conventional joint control

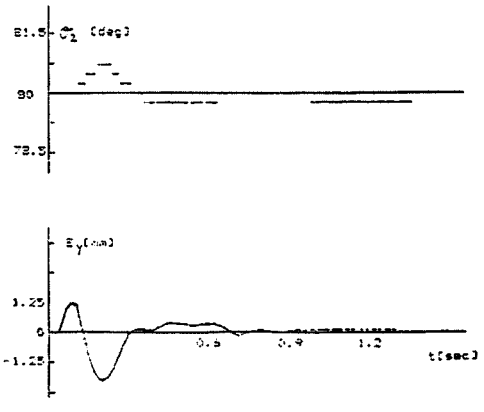

Fig. 5 The arm impulse response with endpoint control

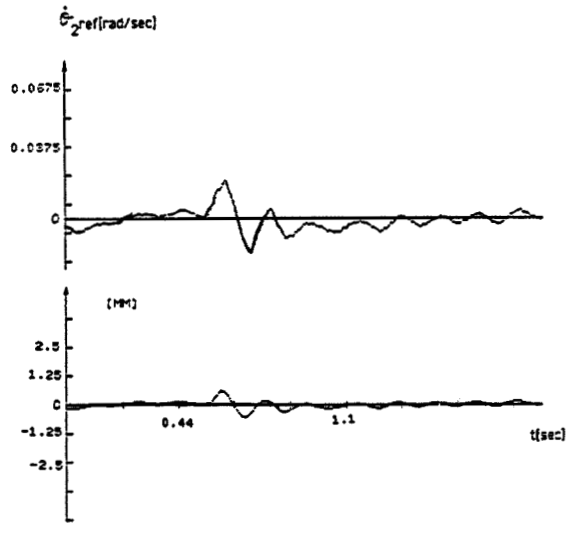

Fig. 6 The reference speed of joint 2 in response to impulse

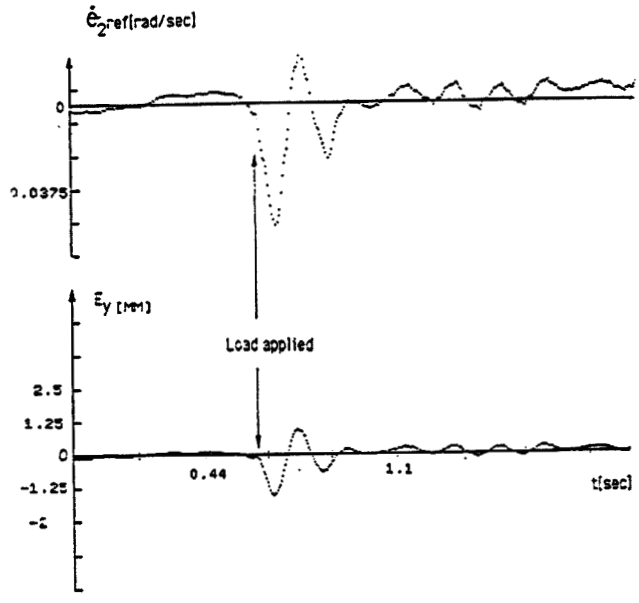

Fig. 9 The reference speed of joint 2 and the error in response to a steady load

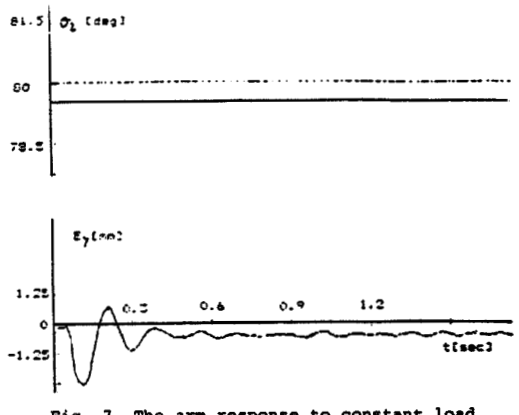

Fig. 7 The arm response to constant load conventional (joint control)

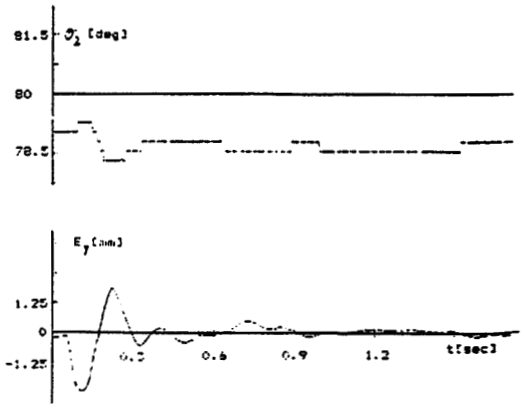

Fig. 8 The arm response to constant load (endpoint control)

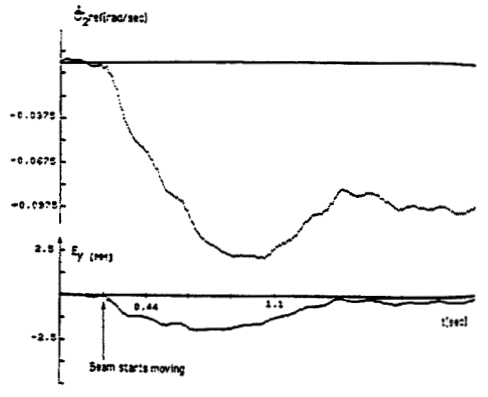

Fig. 10 Arm guided by the beam: error signal and reference signal of joint 2.

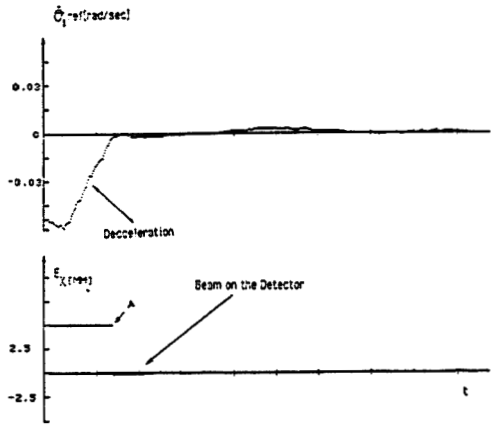

Fig. 11 Decceleration and re-established Contact with the Beam